THE JOURNAL OF BIOLOGICAL CHEMISTRY VOL. 284, NO. 27, pp. 18525–18536, July 3, 2009

Plectin Isoform-dependent Regulation of Keratin-Integrin $\alpha6\beta4$ Anchorage via Ca^{2+}/Calmodulin*[S]

Received for publication, December 24, 2008, and in revised form, April 15, 2009 Published, JBC Papers in Press, May 6, 2009, DOI 10.1074/jbc.M109.008474

Julius Kostan, Martin Gregor, Gernot Walko, and Gerhard Wiche[1]

From the Department of Molecular Cell Biology, Max F. Perutz Laboratories, University of Vienna, Vienna A-1030, Austria

The detachment of epithelial cells from the basal matrix during wound healing and differentiation of keratinocytes requires the disassembly of the hemidesmosomal multiprotein adhesion complex. Integrin $\alpha6\beta4$-plectin interaction plays a major role in the formation of hemidesmosomes, and thus the mechanisms regulating this interaction should be critical also for the disassembly process. Here we show that a particular plectin isoform (1a) interacts with the Ca^{2+}-sensing protein calmodulin in a Ca^{2+}-dependent manner. As a result of this interaction, binding of the hemidesmosome-associated plectin isoform 1a to integrin $\beta4$ is substantially diminished. Calmodulin-binding inhibits also the interaction of plectin with F-actin. Further, we found that, during Ca^{2+}-induced keratinocyte differentiation, plectin 1a is first relocated within the cell and later down-regulated, suggesting that Ca^{2+} affects the fate of plectin 1a upon its release from hemidesmosomes. We propose a novel model for the disassembly of hemidesmosomes during keratinocyte differentiation, where both, binding of calmodulin to plectin 1a and phosphorylation of integrin $\beta4$ by protein kinases, are required for disruption of the integrin $\alpha6\beta4$-plectin complex.

Basal cell layer keratinocytes of the skin are firmly attached to the underlying basement membrane through hemidesmosomes (HDs),[2] protein complexes that mediate stable anchoring by providing a tight link between the intracellular intermediate filament network (IF) system and the extracellular matrix (1, 2). Plectin, a universal and functionally versatile cytolinker protein, has been implicated in HD functions since early on (3, 4). Binding of plectin to the $\beta4$ subunit of integrin $\alpha6\beta4$ turned out to be a critical step in the formation of HDs, and various regions of plectin have been shown to be involved in this interaction. One of them is a canonical actin-binding domain (ABD) of the tandem calponin homology (CH) domain type (5–7), which binds to the second fibronectin type III (FnIII) domain of the $\beta4$ subunit. Residues crucial for this binding are clustered on the surface of the first N-terminal calponin homology domain. They partially overlap with one of the essential F-actin-binding sequences, providing a structural basis for the competitive nature of plectin binding to integrin $\beta4$ and F-actin (2, 8). A second integrin $\beta4$-binding site, located in the plakin domain of plectin (9), interacts with sequences downstream of the second FnIII domain of integrin $\beta4$ (10). In addition, interactions of the C-terminal repeat domain R6 of plectin with the segment connecting the second and third FnIII domains of integrin $\beta4$ (C-segment), and with integrin $\beta4$ tail domain, have been reported (9).

In accordance with plectin being a prominent constituent of HDs, abnormalities in its expression in humans lead to epidermolysis bullosa simplex associated with muscular dystrophy, manifesting as severe skin blistering and muscle disorders (for review see Ref. 11); an autosomal dominant form of the disease (epidermolysis bullosa simplex-Ogna) manifests just in skin (12). Conventional, as well as conditional (K5-Cre-driven) plectin knockouts in prenatal mice led to the death of animals, 2–3 days after birth (13, 14), whereas after induced disruption of the plectin gene in the skin of adult mice, keratinocyte fragility and lesional epidermal barrier defects were reported (14).

The versatile cross-linking and scaffolding abilities of plectin are augmented by the unusual 5′ complexity of its transcripts generated by differential splicing of at least 11 alternative first exons (15). Although the precise function(s) of the various N-terminal sequences of plectin have not been fully elucidated, some of the isoform-specific sequences have been shown to direct the protein to distinct cellular locations, such as HDs, microtubules, mitochondria, costameres, and Z-disks (16–20). Of two major plectin isoforms expressed in primary keratinocytes (plectins 1a and 1c) only plectin 1a, however, anchors keratin IFs to HDs, while plectin 1c was found to co-localize with microtubules (16).

The assembly and disassembly of HDs play an important role in keratinocyte migration during wound healing, differentiation, and carcinoma invasion, yet the mechanisms that control HD dynamics are not fully understood. Several growth stimuli, including epidermal growth factor (EGF) and macrophage stimulating protein, have been implicated in the regulation of HD disassembly, and phosphorylation of integrin $\beta4$ by its effector molecule protein kinase C (PKC) leads to partial disassembly of HDs (for review see Ref. 21). In addition, it has been shown that phosphorylation of integrin $\beta4$ involving tyrosine protein kinase Fyn plays a role in HD disassembly (22). However, the diversity of plectin-integrin-binding sites points toward a more complex regulation, especially as the predicted phosphorylation sites on integrin $\beta4$ map to the C-segment (2,

* This work was supported by the Austrian Science Research Fund (Grant P20744-B11) and from Dystrophic Epidermolysis Research Association, UK.

[S] The on-line version of this article (available at http://www.jbc.org) contains supplemental Figs. S1–S3.

[1] To whom correspondence should be addressed. Tel.: 43-1-4277-52851; Fax: 43-1-4277-52854; E-mail: gerhard.wiche@univie.ac.at.

[2] The abbreviations used are: HD, hemidesmosome; ABD, actin-binding domain; BPAG, bullous pemphigoid antigen; CaM, calmodulin; CCB, Coomassie Brilliant Blue; CH, calponin homology; EGF, epidermal growth factor; F-actin, filamentous actin; FnIII, fibronectin type III domain; GFP, green fluorescent protein; IF, intermediate filament; K5, keratin 5; MBP, maltose-binding protein; PKC, protein kinase C; mAb, monoclonal antibody; 1aABD, 1cABD, and 1fABD, N-terminal fragments of plectin comprising the ABD and the preceding isoform-specific sequences of plectin 1a, plectin 1c, or plectin 1f, respectively.

23), presumably leaving other major binding interfaces, such as that between ABD of plectin and the second FnIII domain, unaffected. Ca^{2+} has the potential to be such an additional regulator. It has an established role in the normal homeostasis of mammalian skin and serves as a modulator in keratinocyte proliferation and differentiation. In fact, Ca^{2+} has been reported to induce the cellular redistribution of the hemidesmosomal protein, BPAG-2 (24), and integrin $\alpha6\beta4$ has been found to be down-regulated during Ca^{2+}-induced differentiation of cultured keratinocytes (25).

In this study, we investigated whether plectin functions are affected by Ca^{2+}. We found that Ca^{2+}-induced differentiation of keratinocytes leads to a redistribution and down-regulation of plectin, similar to that reported for integrin $\alpha6\beta4$. Furthermore we identified plectin as a calmodulin (CaM)-binding protein and showed that the interaction of both proteins is not only strictly Ca^{2+}-dependent, but also plectin isoform-dependent. Our data indicate that CaM binding to plectin 1a, the HD-associated plectin isoform, impedes its interaction with integrin $\alpha6\beta4$ and consequently is likely to play an important role in HD disassembly.

EXPERIMENTAL PROCEDURES

Plasmids and cDNA Constructs—Expression plasmids for integrin $\beta4$ fragments with N-terminal His tags and for plectin fragments fused N-terminally to maltose-binding protein (MBP), have been described previously (9, 15). cDNAs for plectin fragments corresponding to exons 2–5 (CH1), 2–8 (ABD), 1c-8 (1cABD), 1f-8 (1fABD), and 1a-8 (1aADB) were engineered based on published sequences (15), with ends containing suitable restriction sites. For the bacterial expression of proteins with N-terminal His tags, or of untagged proteins, PCR products were subcloned into pBN120 (26), or pGR66 (7), respectively, both of which are derivates of pET-15b (Novagen). All MBP fusion proteins were expressed using vector pMal-c2 (New England Biolabs). Expression plasmids encoding C-terminally GFP-tagged versions of full-length plectin isoform 1a and 1f have been described previously (17, 27). An expression plasmid encoding C-terminally mCherry-tagged CaM was generated by subcloning cDNA for human CaM gene III (a generous gift from Donald C. Chang) into pEGFP-N2 (Clontech Laboratories, Inc.)-based plasmid pGB7 (kindly provided by Gerald Burgstaller), where enhanced GFP had been replaced by mCherry. The mCherry-containing plasmid was kindly provided by Victor J. Small.

Antibodies—For immunoblotting, the following primary and secondary antibodies were used: affinity-purified (isoform-specific) rabbit antibodies to plectin 1c (16), and to plectin 1a (9); mAbs LP34 (DakoCytomation) to K5, K6, and K18 (pan-keratin), anti-K5 and anti-involucrin antisera (PRB-160P and PRB-140C, respectively, Covance), rabbit anti-integrin $\beta4$ antiserum (H-101, Santa Cruz Biotechnology), anti-phospho (Thr-638/641) PKCα/βII antiserum (Cell Signaling Technology, Inc.), mAbs to calmodulin (Upstate), mAbs B-5-1-2 to tubulin (Sigma-Aldrich), goat anti-rabbit IgG and goat anti-mouse IgG, conjugated to horseradish peroxidase or alkaline phosphatase (all from Jackson ImmunoResearch Laboratories). For immunofluorescence microscopy the following primary antibodies were used: anti-plectin 1a antibodies (see above) and rat mAbs to integrin $\alpha6$ (CD49f, BD Biosciences). As secondary antibodies, we used fluorescein isothiocyanate-coupled goat anti-rat IgG and Rhodamine red-X-coupled goat anti-rabbit IgG (both from Jackson ImmunoResearch Laboratories), Alexa Fluor 488-coupled goat anti-rabbit IgG (Invitrogen), and Texas Red-conjugated goat anti-rat IgG (Accurate Chemical & Scientific Corp.). For immunoprecipitation antiserum to plectin number 46 (16) was used.

RNase Protection Assay and Immunoblotting—Isolation of total RNA, RNase protection analysis, and quantification of relative signal intensities were performed as described previously (16). For SDS-PAGE, transfer, and detection of proteins, protocols given in Rezniczek *et al.* (28) were followed.

Cell Culture, Keratinocyte Differentiation, Immunofluorescence Microscopy, and Transient Transfection—Primary mouse keratinocytes were isolated and cultured according to the protocol described by Osmanagic-Myers *et al.* (27), with the exception that dispase (5 units/ml) was used at 37 °C (1 h) to separate epidermis and dermis. Cultures prepared by this protocol routinely comprised 10% of melanocytes. Keratinocytes were identified by positive integrin $\alpha6$ staining. Immortalized wild-type and plectin-deficient mouse keratinocytes were routinely cultured in KGM (Cambrex) on collagen I-coated (Sigma-Aldrich) plastic dishes as described (16). Confluent primary or immortalized (passage numbers 10–15) cultures of keratinocytes, were induced to differentiate by cultivation in medium containing 1.3 mM $CaCl_2$ for up to 5 days. Differentiated keratinocytes were methanol-fixed, immunolabeled, washed with phosphate-buffered saline, mounted in Mowiol, and viewed in a laser-scanning microscope (LSM 510, Carl Zeiss MicroImaging, Inc.) using either Plan-Apochromat 63× (1.4 numerical aperture), or 100× (1.4 numerical aperture) objective lenses (Carl Zeiss MicroImaging, Inc.). LSM software and Photoshop CS2 (Adobe) software package were used for imaging and processing. Transient transfections were performed with subconfluent cultures of immortalized plectin-deficient keratinocytes, using FuGENE reagent (Roche Applied Science) according to the manufacturer's instructions.

Quantitation of HD-like Structures and Their Co-localization with Plectin—For quantitative measurements of the areas covered by HD-like structures and estimation of their co-distribution with plectin, images of immunostained keratinocytes from three independent differentiation experiments were obtained using a 63× objective under constant acquisition settings avoiding pixel saturation. To eliminate noise and background artifacts and to smooth sharp edges of stained structures, merged RGB confocal microscopy images (green and red channels showing integrin $\alpha6$ and plectin 1a staining, respectively) were processed with a 2×2 median filter. To measure cellular surface areas *versus* HD-positive areas (defined by integrin $\alpha6$ staining), two best-fit lower thresholds were determined from 8-bit images of the red channel, using the threshold tool of open source software ImageJ (W. S. Rasband, NIH) and confirmed by visual inspection. HD-positive areas were calculated as percentage of total cell areas. For statistical evaluation of plectin 1a co-localization with integrin $\alpha6$-positive HD-like structures we evaluated merged 8-bit images using the Co-localization High-

lighter plug-in of ImageJ. Prior to co-localization analyses threshold settings for each 8-bit image (red or green) were determined by careful manual thresholding and then assigned to the input window of the Co-localization Highlighter plug-in. The intensity ratio of co-localized pixels was set at 50%. Highlighted areas of maximal co-localization overlapping with previously determined HDs (see above), were scored as co-localizing and calculated as a percentage of HD areas.

Preparation of Cell Fractions—To prepare total cell lysates, differentiated keratinocytes were washed twice with phosphate-buffered saline and lysed directly with 50 mM Tris-HCl, pH 6.8, 100 mM dithiothreitol, 2% SDS, complete mini protease inhibitor mixture (Roche Applied Science), 1% bromphenol blue, 5 mM EDTA, and 10% glycerol. Aliquots of cell lysates containing equal amounts of protein were separated by SDS-PAGE and subjected to immunoblotting. Quantitation of bands was performed as previously described (29). Triton X-100 and high salt extract fractions were prepared from keratinocytes according to Toivola *et al.* (30).

Immunoprecipitation—Plectin wild-type and plectin-deficient keratinocytes, with or without 4-h exposure to 1.3 mM $CaCl_2$, were rinsed twice with cold 20 mM Tris, 137 mM NaCl, 2.7 mM KCl, pH 7.5 (Tris-buffered saline), and then lysed in Tris-buffered saline supplemented with 0.5% Triton X-100, 0.1 mM $CaCl_2$, 0.5 mg/ml DNase I (Roche Applied Science), 0.2 mg/ml RNase A (Serva), 1 mM phenylmethylsulfonyl fluoride, 10 mM benzamidine, 10 μg/ml aprotinin, 10 μg/ml pepstatin/leupeptin, and phosphatase inhibitor mixture 1 (1:100, Sigma-Aldrich). Cell suspensions were incubated for 10 min at room temperature, and clarified by centrifugation (15,800 $\times$ *g*, 30 min, 4 °C). Lysates were pre-cleared by incubation with protein A-Sepharose beads (25 μl/ml lysate, Amersham Biosciences) for 1 h at 4 °C, followed by centrifugation. Cleared supernatants were incubated with antiserum to plectin (number 46) overnight at 4 °C. To recover antibody-antigen complexes, protein A beads were added, and suspensions were rotated for 2 h at 4 °C. Beads were sedimented and washed three times with Tris-buffered saline supplemented with 0.5% Triton X-100 and 0.1 mM $CaCl_2$. Finally, the beads were resuspended in 20 μl of SDS-PAGE sample buffer, heated for 5 min at 95 °C, and subjected to immunoblotting.

Protein Expression and Purification—CaM was prepared from porcine brain (31), actin from rabbit skeletal muscle (32). Recombinant proteins were expressed in *Escherichia coli* BL21(DE3) and purified as described in Reznicek *et al.* (9) (integrin β4 fragments), Fuchs *et al.* (15) (MBP and MBP-tagged proteins), or Sevcík *et al.* (7) (His-tagged and untagged plectin fragments).

Pull-down Assays—For CaM-Sepharose pulldown assays, 50 μl of pre-equilibrated CaM-Sepharose 4B beads (Amersham Biosciences), or of Sepharose 4B alone, were mixed with 1 ml of protein samples (1.5 μM) in 20 mM Tris, 100 mM NaCl, 0.005% Tween 20, pH 7.5, supplemented with either 2 mM $CaCl_2$, or increasing concentrations of $CaCl_2$ (0.4–2000 μM), or 5 mM EGTA, or 2 mM $CaCl_2$ and 80 μM W7 (Fluka), followed by incubation for 2 h at room temperature. Beads were washed three times, and bound proteins were eluted by incubation with SDS-PAGE sample buffer for 10 min at 95 °C.

For 1aABD-Sepharose pulldown assays, purified samples of 1aABD were coupled to CNBr-activated Sepharose 4B (Amersham Biosciences) according to the manufacturers' protocol. 40 μl of these beads was added to samples (1 ml) of β4-$F_{1,2}LF_{3,4}C$, or β4-$F_{1,2}$ (both at 0.5 μM) in 20 mM Tris, 100 mM NaCl, 0.01% Tween 20, pH 7.5 (solution S), supplemented with either 2 mM $CaCl_2$, or 5 mM EGTA. Mixtures were incubated for 1.5 h at room temperature and proteins bound to the beads were analyzed as described above. For competitive binding assays, samples of integrin β4 fragment $F_{1,2}LF_{3,4}C$ (0.5 μM) were mixed with 1aABD-Sepharose beads immediately or 0.5 h before incubation with increasing amounts of CaM (0–10 μM) in a total volume of 1 ml of solution S supplemented with either 0.5 mM $CaCl_2$, or 1 mM EGTA. For determining dissociation constants, increasing concentration of CaM (0–1.26 μM) or β4-$F_{1,2}LF_{3,4}C$ (0–1.13 μM) were mixed with constant amounts of 1aABD-Sepharose (30 μl). After incubation for 1.5 h at room temperature, supernatant (free) fractions were removed by centrifugation at 1,500 $\times$ *g* for 1 min at 20 °C. Beads were washed three times, and proteins in the resultant pellet and supernatant fractions were analyzed by SDS-PAGE. CBB-stained protein bands were quantitated using ImageQuant 5.1 software package (Molecular Dynamics). The amount of CaM or β4-$F_{1,2}LF_{3,4}C$ bound to 1aABD-Sepharose was fit to a single rectangular hyperbola using Prism 4 (GraphPad Software).

Actin Co-sedimentation Assay—Samples of purified rabbit skeletal actin (16 μM) in 20 μl of 5 mM Tris, 0.2 mM $CaCl_2$, 0.2 mM ATP, 0.5 mM dithiothreitol, pH 8, were polymerized by addition of 1/10 volume of 50 mM Tris, 0.5 M KCl, 20 mM $MgCl_2$, 20 mM ATP, pH 8, and incubation for 1 h at room temperature. Preincubated mixtures (30 min, room temperature) of 8 μM purified 1aABD (or 1fABD) and 0–160 μM CaM in 20 μl of 5 mM Tris, 50 mM KCl, 2 mM $MgCl_2$, 2 mM ATP, pH 8 (supplemented with either 4 mM $CaCl_2$, or 10 mM EGTA) were added to polymerized actin samples and incubated for another 30 min. Actin filaments and proteins bound were sedimented by centrifugation (217,000 $\times$ *g*, 30 min, 20 °C), and equivalent volumes of the supernatant and pellet fractions were analyzed by SDS-PAGE. CBB-stained protein bands were quantitated using the ImageQuant 5.1 software package (Molecular Dynamics). For determining dissociation constants, the same assay has been used, except that increasing concentrations of 1aABD or 1fABD (0–130 μM) were mixed with constant amounts of actin (8 μM). The amount of 1aABD or 1fABD bound to F-actin was fit to a single rectangular hyperbola using Prism 4 (GraphPad Software).

Dot Blot Assay—Fragment 1aABD was labeled with Alexa Fluor®680 using a Protein Labeling Kit (Molecular Probes) according to the manufacturers' instructions. Purified recombinant His-tagged fusion proteins containing integrin β4 fragments, as well as 1aABD, were dialyzed overnight against 20 mM Tris, 0.2% glycerol, 100 mM NaCl, 0.5 mM dithiothreitol, pH 7.5 (solution P), and subsequently precleared by centrifugation at 100,000 $\times$ *g* for 2 h at 4 °C. Samples were diluted in solution P and spotted (4 μg/spot) onto a nitrocellulose membrane using a Bio-Rad 96-wells dot blot system. Immobilized proteins were incubated with 1% milk in 20 mM Tris, 100 mM NaCl, pH 7.5, for 1 h, or stained with

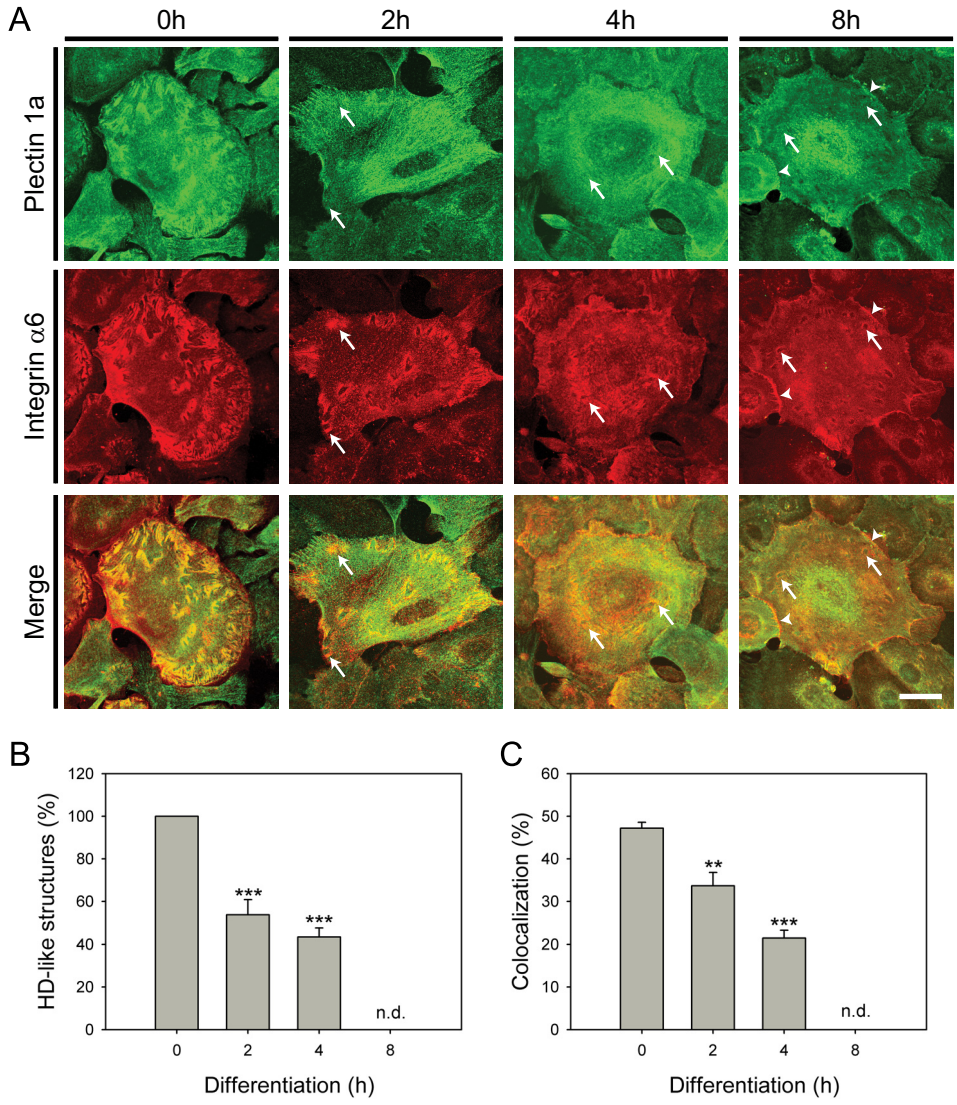

FIGURE 1. **Redistribution of plectin 1a in the early stages of Ca^{2+}-induced keratinocyte differentiation.** *A*, cultures of primary keratinocytes, exposed to Ca^{2+} for 0, 2, 4, and 8 h, were subjected to immunofluorescence microscopy using antibodies indicated. *Arrows* point to areas where plectin 1a staining does not coincide with integrin α6-positive HD-like structures. *Arrowheads* denote areas at the cell periphery with accumulation of plectin 1a. Note, wedge-like patterns typical of HD-like structures in primary keratinocytes. *Bar*, 20 μm. *B* and *C*, *bar diagrams* representing statistical quantitation of HD-like (integrin α6-positive) structures (*B*) and co-localization of plectin 1a with integrin α6 (*C*) in primary keratinocytes during Ca^{2+}-induced differentiation. Data shown in *B* and *C* represent mean values (±S.E.). 15 cells of the type shown in *A* from three different experiments were analyzed; ** and ***, $p < 0.01$ and $p < 0.001$, respectively. *n.d.*, not determined. Note, there is a reduction of HD-like structures, as well as a decrease in co-localization of plectin 1a with integrin α6 in the course of differentiation.

CBB. Samples of 1aABD were diluted to 3 μg/ml in solution S, and incubated with nitrocellulose strips for 1.5 h at room temperature. Strips were then washed three times in solution S, and scanned using an Odyssey Infrared Imager (Li-Cor, Bioscience, Lincoln, NE).

RESULTS

Ca^{2+}-induced Redistribution of Plectin 1a in Differentiating Keratinocytes—In the early stages of keratinocyte differentiation (as well as of wound healing) hemidesmosomal components, such as integrin α6β4 and BPAG-2, show a redistribution from HDs to other cell compartments (24, 33). To examine the fate of HD-associated plectin 1a under similar conditions, confluent cultures of primary mouse keratinocytes were subjected to differentiation by exposure to 1.3 mM $CaCl_2$ for up to 8 h (Fig. 1*A*). Prior to differentiation (0 h), plectin 1a was found associated with prominent integrin α6-positive wedge-like structures. However, only 47% of these structures were also positive for plectin 1a, probably reflecting a heterogeneity of HD-like structures due to differences in their assembly state and/or stability. Interestingly, previous studies with immortalized keratinocyte cell lines cultivated under similar conditions revealed HD-like structures resembling circular Swiss cheese-like patterns rather than wedge-like arrangements (16) (see also supplemental Fig. S1). Upon Ca^{2+}-induced differentiation of primary keratinocytes, a remarkable redistribution of plectin 1a was observed (Fig. 1*A*). Already within the first 2–4 h of differentiation, the plectin 1a signal became less prominent at HD-like structures, while at the same time the protein became diffusely distributed within the cell, showing an accumulation in peripheral cell-cell contact areas as well as in perinuclear regions, as differentiation proceeded (Fig. 1*A*, *arrowheads*). Integrin α6 showed a similar redistribution to the cell margins, accompanied by a reduction of HD-like structures in the cell interior (Fig. 1, *A* and *B*). A quantitative analysis revealed that already 2 h after addition of Ca^{2+}, the amount of HD-like structures was reduced to 53% of control values (0 h), with a further drop to 43% after 4 h of differentiation (Fig. 1*B*). HD-like structures, which were still noticeable at later stages of Ca^{2+} treatment (8 h), in general were plectin 1a-negative (Fig. 1*A*, *arrows*). The amount of plectin 1a/integrin α6-costained structures after 4 h of Ca^{2+} treatment was reduced to less than half compared with untreated cells (0 h) (Fig. 1*C*), implying dissociation of plectin 1a from integrin α6β4 and HD-like structures during the differentiation process. Except for the shape of HD-like structures, similar observations were made using immortalized mouse keratinocyte cell cultures instead of primary cells (data not shown).

Plectin 1a Is Down-regulated during Long Term Differentiation of Keratinocytes—Ca^{2+}-induced differentiation of cultured keratinocytes leads to down-regulation of integrin α6β4,

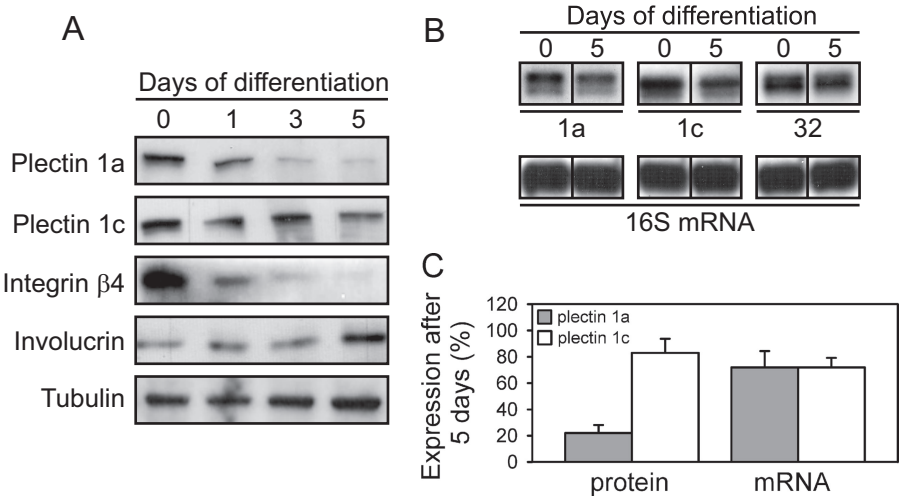

FIGURE 2. **Down-regulation of plectin 1a during Ca^{2+}-induced differentiation of keratinocytes.** *A*, immortalized mouse keratinocytes were left undifferentiated (0), or were differentiated for 1, 3, and 5 days in medium containing 1.3 mM $CaCl_2$. Cells were lysed, and extracts were analyzed by immunoblotting using antibodies to proteins indicated. Tubulin levels served as loading controls. *B*, RNase protection assays of plectin transcripts containing distinct first coding exons in undifferentiated (0 days), or 5-day-differentiated keratinocytes. Total RNA was analyzed using Riboprobes specific to exons 1a, 1c, and 32. A murine ribosomal protein S16 mRNA probe was used as loading control. Fragments protected are shown. *C*, relative protein and mRNA levels (percentages) of plectin 1a and plectin 1c in 5-day-differentiated compared with undifferentiated (100%) keratinocytes. Data represent mean values (±S.E.) of three independent experiments. Note more rapid decrease of plectin 1a protein content in comparison to its mRNA level within 5 days of differentiation.

initially through proteolytic cleavage of both subunits, followed by repression of integrin gene expression (25). This suggests that post-transcriptional regulation of integrin $\alpha6\beta4$ is a primary consequence of cell differentiation commitment. As we found that plectin 1a becomes redistributed within keratinocytes already during the initial stages of differentiation, we speculated that it, too, might be down-regulated in the course of differentiation. To test this hypothesis, immortalized mouse keratinocytes were grown until confluency in medium with low Ca^{2+} content (0.05 mM) and were then allowed to differentiate for several days in medium containing 1.3 mM Ca^{2+}. When we prepared total cell lysates at different time points of differentiation and monitored by immunoblotting the expression of plectin 1a, integrin $\beta4$, involucrin, and plectin 1c, another isoform of plectin expressed in keratinocytes (16), we found the expression of integrin $\beta4$ and plectin 1a to be substantially decreased already during the first day of differentiation (Fig. 2*A*). After 5 days, the amount of plectin 1a was reduced by 78%, while that of plectin 1c was decreased only by 20% during the same time period (Fig. 2*C*). The expression of involucrin (a terminal differentiation marker), as expected, was increased (Fig. 2*A*), whereas no changes were observed in tubulin expression levels, serving as loading controls (Fig. 2*A*). Similar data were obtained using primary mouse keratinocytes instead of immortalized cell cultures (data not shown). When transcript levels were assessed using RNase protection assays with antisense Riboprobes specific for exons 1a (plectin 1a), 1c (plectin 1c), or 32 (total plectin), and ribosomal protein S16 (internal control), plectin 1a and plectin 1c mRNA levels were found equally reduced (to 70%) after 5 days of differentiation (Fig. 2, *B* and *C*). Transcript levels of total plectin were found reduced to ~90% (Fig. 2*B*). Thus, Ca^{2+} elevation led to a loss of transcripts for both plectin isoforms, although at least in the case of plectin 1a this loss occurred at a lesser rate at the transcript, compared with the protein level (Fig. 2*C*). Hence, expression of plectin 1a in differentiating keratinocytes was subject to transcriptional as well as post-transcriptional regulation, similar to integrin $\alpha6\beta4$.

Association of CaM with Plectin 1a upon Ca^{2+}-triggered Differentiation of Keratinocytes—Because the phosphorylation of integrin $\beta4$ by PKCα caused only a partial disassembly of HDs (23, 34), we figured, additional mechanism might be required for their complete disassembly. The PKCα activator Ca^{2+} also activates CaM, a ubiquitous Ca^{2+}-sensing protein, that is known to modulate some of the functions of dystrophin, utrophin, and filamin through its direct binding to their highly conserved ABDs (35–37). Because plectin shares a similar ABD (7), it was of interest whether plectin 1a, too, binds to CaM and whether such an interaction could affect plectin-mediated IF network anchorage at HDs. To address these issues, we first prepared 1% Triton X-100 soluble and insoluble (cytokeratin-enriched) subcellular fractions from differentiating cultured keratinocytes, and subjected them, along with total cell lysates, to immunoblotting using antibodies to integrin $\beta4$, plectin 1a, CaM, PKCα/βII, and keratin 5 (K5), or pan-keratin (K5, K6, and K18) (Fig. 3, *A* and *B*). The relative amounts of detectable keratins and phosphorylated (activated) PKCα/βII served as controls for equal loading and as a differentiation marker, respectively. The analysis of total cell lysates at various time points revealed hardly any differences in the expression profiles of these proteins during Ca^{2+}-induced differentiation (Fig. 3*A*). As expected, the relative distribution of cytokeratins, most of which were found in the insoluble fractions, was hardly altered during the early stages of differentiation (Fig. 3*B*). As revealed by densitometric analysis, integrin $\beta4$ became more prominent in the soluble fraction with continuing differentiation (Fig. 3, *B* and *C*), probably as a result of increased phosphorylation by PKCα leading to its reduced association with the keratin filaments. Unlike integrin $\beta4$, plectin 1a was found predominantly in the cytokeratin-enriched fraction during the first 4 h of differentiation while becoming somewhat more soluble only after 8 h (Fig. 3, *B* and *C*). This suggested that plectin, in contrast to integrin $\beta4$, remained associated with insoluble keratin filaments, at least during the early phases of differentiation. The same seemed to apply to CaM, as it, too, was found to co-distribute with the insoluble cytokeratin fraction, especially at the 2- and 4-h time points (Fig. 3, *B* and *C*).

To assess a possible molecular interaction of plectin and CaM, subconfluent cultures of plectin-deficient (null) mouse keratinocytes were co-transfected with expression plasmids

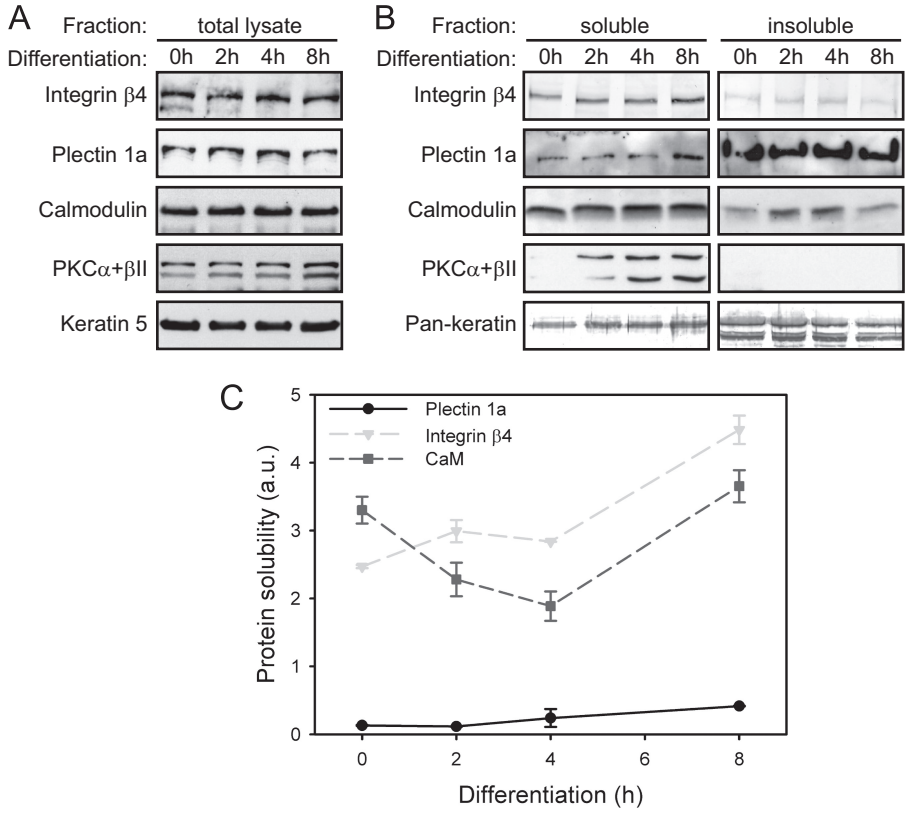

FIGURE 3. **Increased association of CaM with the insoluble cytokeratin fraction in the course of Ca^{2+}-induced keratinocyte differentiation.** Immortalized mouse keratinocytes were grown on collagen I and either left untreated (0 h), or stimulated with $CaCl_2$ for 2, 4, and 8 h. *A*, cells were lysed without extraction (total lysate) and analyzed by immunoblotting using antibodies to proteins indicated. *B*, cells were sequentially extracted to obtain Triton-soluble (*soluble*) and cytokeratin-enriched (*insoluble*) fractions, and analyzed as in *A*. Keratin levels assessed by keratin 5 (*A*), or anti-pan-keratin (*B*) antibodies, served as loading controls. *C*, quantitation of protein solubility at different time points of differentiation. Signal intensities of plectin 1a, integrin *β4*, and CaM in soluble and insoluble fractions were quantified by densitometry of gels, including the one shown in *A*. Data points represent ratios between amounts of protein in soluble *versus* insoluble fractions. Mean values (±S.E.) of three independent experiments are shown. In some cases, *error bars* do not extend outside of data point symbols. Note that there was a decrease of CaM solubility within 2 and 4 h of differentiation.

encoding mCherry-CaM and GFP-mouse plectin isoform 1a (full-length) fusion proteins. Upon exposure to Ca^{2+} for 4 h, keratinocytes were extending small lamellipodia and/or ruffles (Fig. 4*A*). In these cells, GFP-plectin 1a showed a rather diffuse localization throughout the cytoplasm, with an accumulation at the cell periphery in areas resembling lamellipodia (Fig. 4*A*, *upper row*, *arrows*). As expected, mCherry-CaM was mostly found evenly distributed throughout the cytoplasm (Fig. 4*A*); the only clearly discernible structures with which CaM associated were lamellipodial ruffles, strikingly similar to plectin 1a (Fig. 4*A*, *arrows*). Ca^{2+}-dependent co-localization of plectin 1a and CaM was observed also in rat bladder carcinoma 804G cells and in wild-type mouse keratinocytes, upon tracing the endogenous proteins using specific antibodies (data not shown). To assess the influence of alternative first exon-encoded sequences on plectin-CaM co-distribution, we co-expressed mCherry-CaM with GFP-tagged full-length mouse plectin isoform 1f (instead of isoform 1a) in plectin-null keratinocytes. Compared with plectin 1a, plectin 1f displayed a slightly more pronounced filamentous phenotype (Fig. 4*A*), indicating its association with actin-stress fibers and most likely focal adhesion contacts, as previously reported (17). The overall distribution of CaM in these cells was similar to that in cells expressing plectin 1a; however, co-localization of CaM with plectin 1f in ruffles of lamellipodia was much less pronounced (if at all noticeable) compared with plectin 1a, indicating specific association of CaM with plectin 1a (Fig. 4*A*). This notion was confirmed by a statistical evaluation of cells displaying plectin 1a- and plectin 1f-CaM co-localization in lamellipodia (Fig. 4*B*). As expected, plectin 1a-CaM co-localization was found in 64% of Ca^{2+}-differentiated keratinocytes, whereas in the case of plectin 1f this was true for only 29% of the cells. The difference in co-localization of CaM with these two isoforms of plectin was even more pronounced in differentiated wild-type keratinocytes (data not shown).

Finally, when plectin was immunoprecipitated from lysates of wild-type keratinocytes differentiated for 4 h, CaM partially co-sedimented with plectin (Fig. 5*A*, +/+, 4 h), whereas in corresponding fractions from undifferentiated keratinocytes (Fig. 5*A*, +/+, 0 h), or from plectin$^{-/-}$ cells (Fig. 5*A*, −/−, 4 h), CaM could not be detected. Thus, subcellular fractionation, co-transfection, and co-immunoprecipitation data combined, provided strong evidence for Ca^{2+}-induced association of plectin with CaM during the initial period of keratinocyte differentiation.

Plectin Interacts with CaM via Its CH1 Domain in a Ca^{2+}- and Isoform-dependent Manner—Based on *in silico* predictions of CaM-binding amphiphilic α-helices, pulldown experiments (filamin A), and overlay assays (dystrophin), the putative CaM-binding site of dystrophin, utrophin, and filamin A were assigned to a region lying within the CH1 domains of their ABDs (36–38). To test, whether plectin interacted with CaM via a similar domain, we performed pulldown assays, with Sepharose-bound CaM (*CaM-S*) and recombinant versions of the ABD of plectin, or its CH1 domain, both N-terminally fused to MBP; MBP alone and Sepharose beads without bound CaM (*S*) were used as controls. When tested in the presence of either 2 mM $CaCl_2$, or 5 mM EGTA, neither the ABD of plectin nor MBP alone showed binding to CaM-Sepharose (Fig. 5*B*). In contrast, the CH1 domain of plectin showed strong binding to CaM in the presence of Ca^{2+}, but not in its absence (Fig. 5*B*). No binding of the CH1 fusion protein to Sepharose beads without bound CaM was observed. Furthermore, in the presence of W7, a specific inhibitor of CaM, binding of the CH1 fusion protein to CaM-Sepharose was substantially diminished. These experiments confirmed the Ca^{2+}-dependent association of CaM

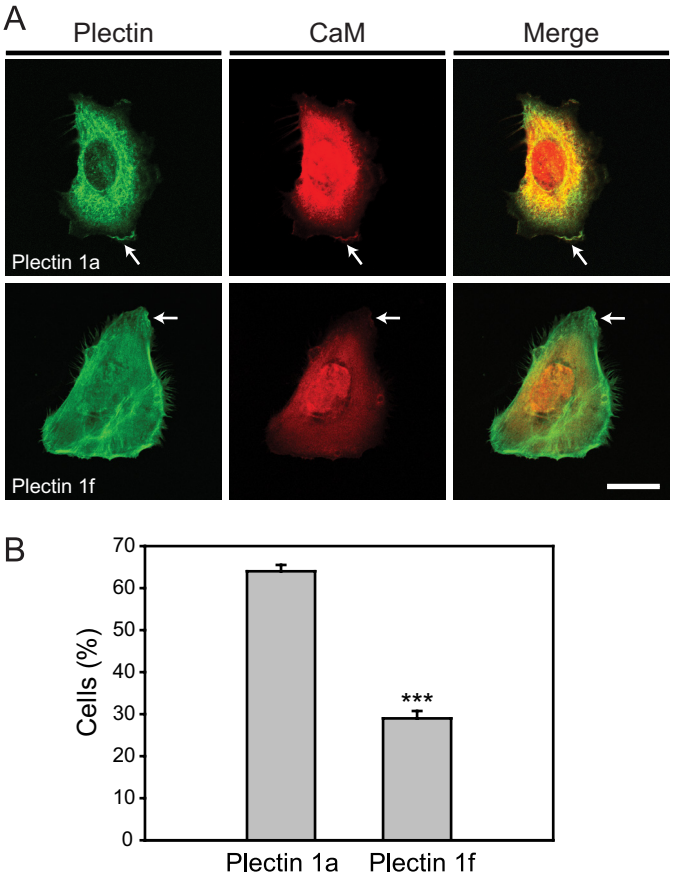

FIGURE 4. **Co-localization of plectin and CaM during early stages of Ca^{2+}-induced keratinocyte differentiation.** *A*, immortalized plectin-deficient keratinocytes co-transfected with full-length GFP-tagged plectin isoforms 1a or 1f (*plectin*), and mCherry-tagged CaM (*CaM*), were differentiated for 4 h in the presence of 1.3 mM $CaCl_2$. *Arrows* denote lamellipodial ruffles. *Bar*, 20 μm. *B*, statistical evaluation of primary keratinocytes displaying plectin 1a- and plectin 1f-CaM co-localization during Ca^{2+}-induced differentiation. Data shown represent mean values (±S.E.). More than 70 cells of the type shown in *A* from three different experiments were analyzed; ***, $p < 0.001$.

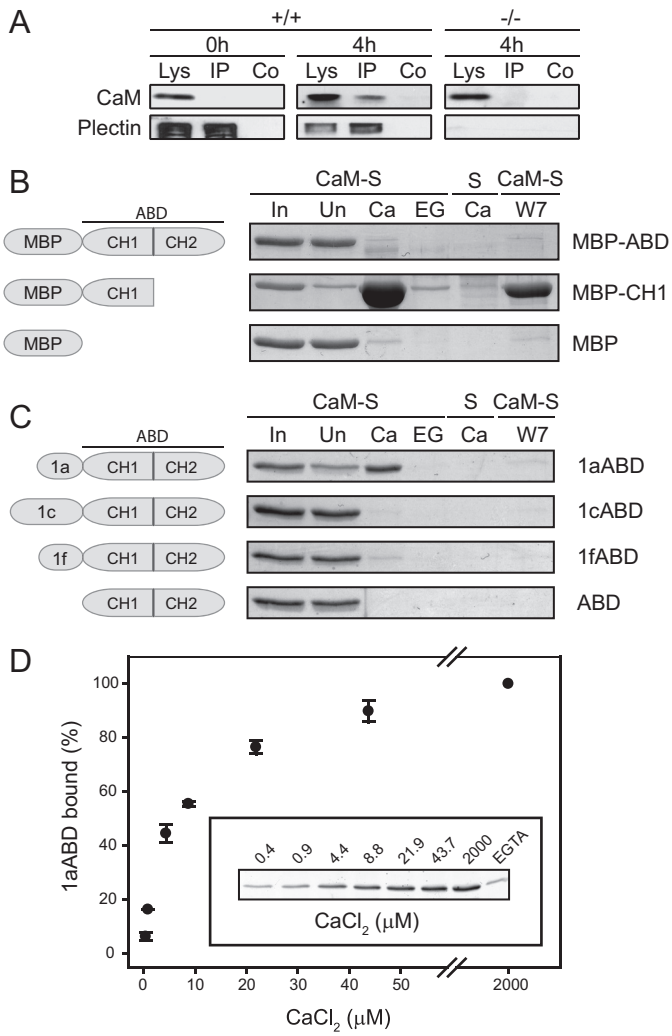

FIGURE 5. **Ca^{2+}- and isoform-dependent interaction of plectin with CaM.** *A*, lysates (*Lys*) from undifferentiated (0 h) or differentiated (4 h) immortalized mouse wild-type (+/+) and plectin-null (−/−) keratinocyte cultures were incubated with anti-pan plectin antibodies (*IP*), or without antibodies (*Co*). Immunocomplexes formed were sedimented using protein A beads, and the precipitates were subjected to immunoblotting using antiserum to plectin 1a or CaM. Note, partial co-sedimentation of CaM with plectin is seen only in lysates from differentiated wild-type keratinocytes. *B*, fusion proteins of MBP with the ABD of plectin (*MBP-ABD*), or N-terminal CH1 domain (*MBP-CH1*), or MBP alone (*MBP*), were incubated with CaM-Sepharose beads (*CaM-S*), or empty beads (*S*), in the presence of 2 mM $CaCl_2$ (*Ca*), or 5 mM EGTA (*EG*), or a mixture of 2 mM $CaCl_2$ and 80 μM W7 (*W7*). After washing of beads, proteins bound were analyzed by SDS-PAGE. ~3% of input (sample supplemented with 2 mM $CaCl_2$ before addition of CaM-Sepharose beads) and of unbound protein fractions (after pulldown) were analyzed in lanes *In* and *Un*, respectively. Proteins were visualized by staining with CBB. *C*, as *B*, using untagged versions of the ABD of plectin, preceded by plectin isoform 1a-, 1f-, and 1c-specific sequences, and of the ABD alone, instead of MBP fusion proteins. Note, that only MBP-CH1 and 1aABD showed binding to Ca^{2+}/CaM. Schematic representations in *B* and *C* show protein fragments used in the assays. *D*, Ca^{2+}-dependent binding of 1aABD to CaM-Sepharose. Pull-down assays with 1aABD were performed as in *B*, except that increasing concentrations of $CaCl_2$ were used as indicated. The relative amount of 1aABD that bound to CaM was determined by densitometry and plotted subtracting the amount of protein sedimented in the presence of 5 mM EGTA (*EGTA*). Data are presented as percentage of binding compared with maximum (100%) 1aABD binding in the presence of 2 mM $CaCl_2$. Mean values (±S.E.) of three independent experiments are shown.

with plectin detected *in vivo*. The observation that the ABD of plectin did not show CaM binding (albeit containing the CH1 domain), whereas the CH1 domain alone did, suggested that the CaM-binding site residing in the MBP-ABD fusion protein was inaccessible, and a conformational change of the ABD of plectin was probably required for CaM binding.

Because plectin comprises an unusually high number (about a dozen) of alternatively spliced first exons, all of which precede the ABD-encoding exons 2–8, there is the intriguing possibility that the various first exon-encoded sequences affect the binding activities of the ABD. To test this, we subjected N-terminal fragments of plectin comprising the ABD, and the preceding isoform-specific sequences of either plectin 1a (1aABD), plectin 1c (1cABD), or plectin 1f (1fABD), together with the ABD without any preceding sequence (ABD), to pulldown assays using CaM-Sepharose. Interestingly, only fragment 1aABD showed binding to CaM-Sepharose beads, whereas no, or hardly any, binding was observed for the other fragments (Fig. 5*C*). CaM binding of 1aABD was specific, as demonstrated by its dependence on Ca^{2+}, lack of binding to Sepharose without bound CaM, and abolishment of binding in the presence of W7. When monitoring the calcium dose response (0.4 μM to 2 mM $CaCl_2$) of 1aABD binding to CaM-Sepharose, binding was observed down to the lowest calcium concentration tested (Fig. 5*D*). In fact very similar dose-response data were reported for

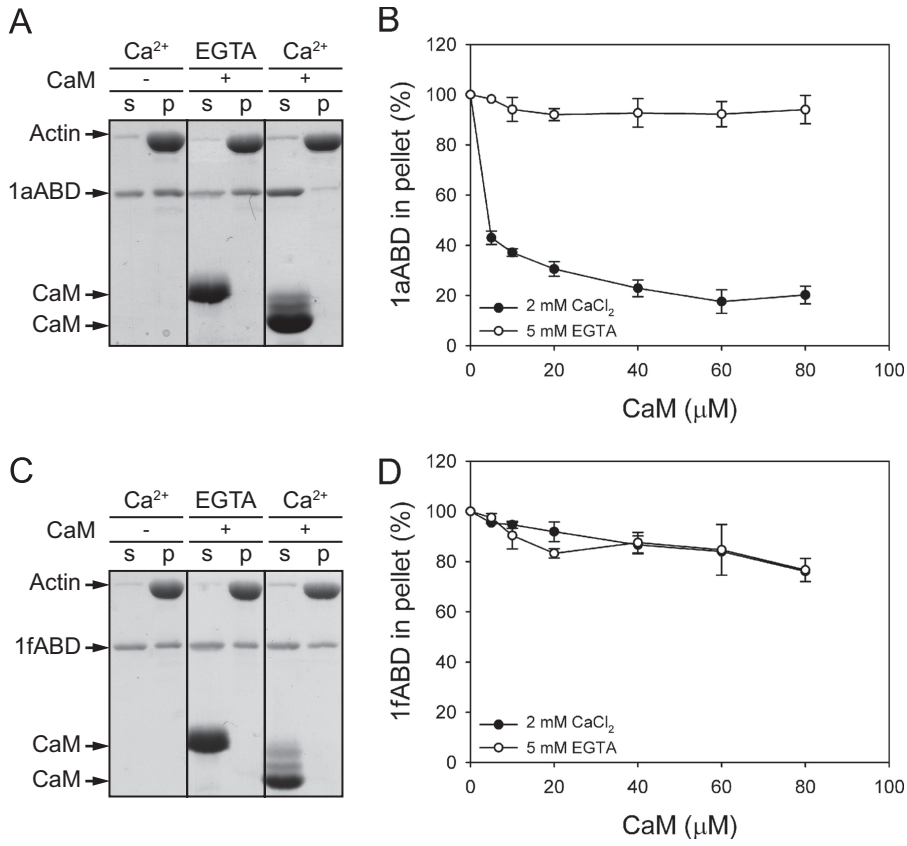

FIGURE 6. **Differential modulation of 1aABD- and 1fABD-F-actin binding by CaM.** *A* and *C*, mixtures of recombinant plectin fragments 1aABD (*A*), or 1fABD (*C*), with or without CaM, were incubated, with preassembled F-actin, in the presence of Ca^{2+}, or EGTA. Actin filaments and proteins bound were sedimented by centrifugation, and equal amounts of supernatant (*s*) and pellet (*p*) fractions were subjected to SDS-PAGE; separated proteins were visualized by CBB staining. *B* and *D*, densitometric quantitation of gel bands, obtained in experiments run under conditions similar to those of *A* and *C*, except that increasing concentrations of CaM were present in the reaction mixtures. Data are presented as percentage of binding compared with maximum (100%) F-actin binding in the absence of CaM. Mean values (±S.E.) of three independent experiments are shown.

filamin A binding to CaM using *in vitro* binding assays and conditions that were similar to those of our study (37).

Ca^{2+}/CaM Regulates Binding of Plectin 1a to F-actin—As a transducer of cytosolic Ca^{2+} signals regulating the activities of proteins, CaM plays a crucial role in a variety of Ca^{2+}-dependent signaling pathways. Investigating the physiological aspects of the specific interaction of CaM with plectin 1a, we next examined the effects of CaM on the binding of plectin to filamentous actin (F-actin) using a co-sedimentation assay. For this, we tested two isoform-specific fragments of plectin that had shown distinct CaM-binding properties, 1aABD and 1fABD. Prior to co-sedimentation with polymerized F-actin, both samples were mixed with increasing concentrations of CaM, in the presence of either 2 mM $CaCl_2$ or 5 mM EGTA. The analysis of supernatant and pellet fractions by SDS-PAGE showed that CaM, in a concentration- and Ca^{2+}-dependent manner, strongly inhibited F-actin binding of 1aABD, but had only minor effects in the absence of Ca^{2+} (Fig. 6, *A* and *B*). In the case of 1fABD, CaM reduced 1fABD-F-actin binding only moderately and independently of Ca^{2+}, suggesting that this interaction was unspecific (Fig. 6, *C* and *D*). This was consistent with the data from pulldown assays where only 1aABD, but not 1fABD, showed binding to CaM (Fig. 5*C*). Considerably larger N-terminal fragments of these isoforms (encoded by exons 1a/1f-24), showed a similar behavior when subjected to co-sedimentation assays, indicating that CaM activities were unaffected and thus independent of plectin sequences flanking the ABD C-terminally (data not shown). To assess the actin-binding affinities of 1aABD and 1fABD, we determined their actin-binding dissociation constant (K_d values) in the absence of CaM, using co-sedimentation assays. As shown in supplemental Fig. S2, both fragments displayed very similar K_d values (6.27 and 7.53 μM for 1aABD and 1fABD, respectively), supporting the notion that the inhibitory effect of CaM on the actin binding of plectin was isoform-specific. We conclude that CaM regulates plectin-actin filament interaction in a Ca^{2+}- and plectin isoform-dependent manner, inhibiting the actin binding of plectin 1a, but not of plectin 1f.

Binding of CaM to Plectin 1a Prevents Association of Plectin with Integrin β4—In light of the ability of CaM to regulate plectin 1a-F-actin binding, it was of interest to assess whether it could also influence plectin interaction with integrin β4, and thus could play a role in the assembly and/or disassembly of HDs. In fact, in previous studies, a binding site for integrin β4 has been mapped to the CH1 domain of plectin and binding of integrin β4 and of F-actin to plectin was shown to be mutually exclusive (8). In addressing this issue, we used untagged N-terminal plectin fragments, as artificial sequences originating from fused tags may influence the conformational flexibility of these fragments with consequences for their binding properties. In a first series of experiments, a panel of soluble integrin β4 fragments (8) (see also Fig. 7 and supplemental Fig. S3) was immobilized on nitrocellulose membranes and overlaid with 1aABD labeled with Alexa Fluor 680. Infrared imaging revealed that 1aABD bound strongly to β4-$F_{1,2}LF_{3,4}C$, β4-$F_{1,2}L'$, and β4-$F_{1,2}L$ but not to any of the other integrin β4 fragments tested (Fig. 7). These data were in accordance with previous studies, showing that the first pair of fibronectin type III domains and part of the connecting segment of β4 were the minimal region required for the interaction of the ABD of plectin with integrin β4 (8). Next, untagged 1aABD immobilized on CnBr-activated Sepharose beads was used to pull down the integrin β4 fragment β4-$F_{1,2}LF_{3,4}C$, in the presence of increasing concentration of Ca^{2+}-bound, or Ca^{2+}-free forms of CaM. As in the case of F-actin, CaM inhibited the association of integrin β4 with 1aABD in a concentration- and strictly Ca^{2+}-dependent man-

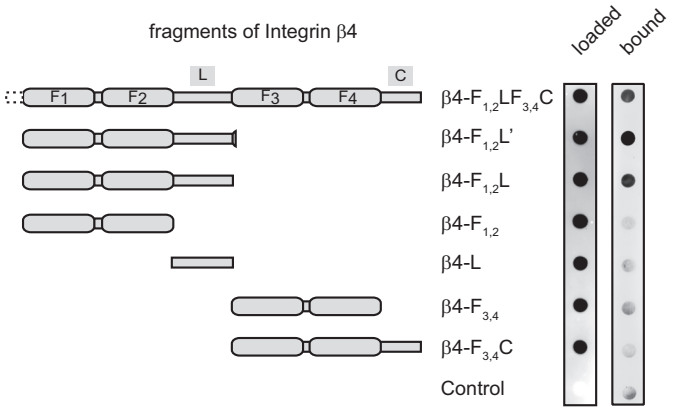

FIGURE 7. **Binding of 1aABD (Alexa Fluor 680-labeled) to recombinant fragments of integrin β4.** Purified His-tagged recombinant proteins (see supplemental Fig. S2), representing the schematically indicated fragments of integrin β4 (for details see Ref. 9), were spotted in duplicates (4 μg each) onto nitrocellulose membranes; solution P (for details see "Experimental Procedures") served as control for unspecific binding and/or background fluorescence (control). One set of membrane-immobilized proteins was stained with CBB as a loading control (*loaded*), the other (*bound*) was overlaid with 1aABD (3 μg/ml), and bound protein was analyzed in an Odyssey infrared imager.

ner (Fig. 8*A*). A quantitative analysis revealed that suppression of integrin β4–1aABD binding by CaM reached 60% under these conditions (Fig. 8*D*). Furthermore, when the integrin β4 fragment was allowed to preform a complex with Sepharose bead-immobilized 1aABD during a 30-min incubation before activated CaM was added, CaM effected a similar disruption of the plectin-integrin complex (Fig. 8, *B* and *D*). Control experiments showed no binding of β4-$F_{1,2}LF_{3,4}C$ to empty beads, nor of β4-$F_{1,2}$ (an integrin β4 fragment that had not shown binding to 1aABD in dot blot assays) to Sepharose bead-immobilized 1aABD or empty beads (Fig. 8*C*). CaM, showing no binding to empty beads, co-sedimented with bead-immobilized 1aABD in a Ca^{2+}-dependent and W7-suppresible manner (Fig. 8*C*). These data clearly established the specificity of the pulldown assay used for assessing competitive binding (Fig. 8, *A* and *B*). Measurements of the dissociation constants of CaM and of the integrin β4-$F_{1,2}LF_{3,4}C$ fragment to 1aABD Sepharose revealed that integrin bound to 1aABD Sepharose with slightly higher affinity (K_d = 0.05 μM) compared with CaM (K_d = 0.16 μM) (Fig. 8*E*). Even though the K_d values measured under these *in vitro* conditions were within a similar range, a locally higher concentration of CaM (compared with plectin) would provide a basis for the successful displacement of plectin 1a from integrin in keratinocytes.

DISCUSSION

Several recent studies revealed that phosphorylation of the integrin β4 subunit plays a role in the disruption of its interaction with plectin (23, 39, 40). Here we show that, in addition, this interaction is regulated by CaM, which prevents integrin β4-plectin association by binding to the ABD of plectin in a Ca^{2+}- and plectin isoform-dependent manner. We propose that this type of regulation is important for the dissociation of plectin from integrin β4 during the early stages of keratinocyte differentiation, with implications for keratinocyte migration and wound healing.

CaM-Plectin Binding Is Regulated by First Exon-encoded Sequences of Plectin—The difference in CaM binding of plectin's entire ABD compared with its CH1 domain could be explained by distinct conformational states of the ABD, with the conformation adopted by plectin isoform 1a being optimal for CaM binding. In fact, two conformational stages of the ABD of plectin and a model for the transition from one stage to the other upon binding to F-actin, have previously been proposed (6). Similarly, a recombinant version of the CH1 domain of filamin A, but neither the full-length protein nor its CH1 domain-containing full-length ABD were found to bind to CaM in the absence of F-actin, suggesting that filamin, too, harbors a cryptic CaM-binding site in its CH1 domain, which becomes exposed upon binding to F-actin (37). Based on our data it is conceivable that sequences encoded by plectin's first exons mediate the conformational change of the ABD required for CaM binding, thereby modulating the function of plectin. In support of this model, we found that an N-terminal fragment of plectin, containing the ABD preceded by exon 1a-encoded sequences, associated with CaM, whereas similar fragments containing plectin 1f- and plectin 1c-specific sequences showed no, or only weak interaction with CaM. Furthermore, our data showed that CaM regulated actin binding of the plectin 1a fragment in an isoform-dependent manner, whereas actin binding in the absence of CaM appeared to be isoform-independent. Moreover, full-length plectin 1f showed substantially reduced co-localization with CaM compared with plectin 1a when expressed in plectin-deficient keratinocytes. ABD-preceding residues corresponding to plectin isoforms 1a and 1c have previously been suggested to affect the binding of the ABD of plectin to integrin β4, because plectin 1c fragments in yeast two-hybrid assays were found to bind to integrin β4 more efficiently than the corresponding fragments of plectin 1a (41). However, these results were inconclusive insofar as only plectin 1a, but not plectin 1c, is recruited to HDs in basal keratinocytes (16), suggesting that the regulation of the interaction of plectin with integrin β4 by CaM may be restricted to plectin isoform 1a in the vicinity of HDs. Interestingly, the two-orders-of-magnitude difference in plectin 1aABD binding affinities to actin and integrin could explain why plectin 1a in keratinocytes shows preferential binding to integrin. On the other hand, our data indicate that N-terminal amino acid sequences do not only influence the binding of the ABD of plectin to integrin β4, but also to F-actin, because the actin-binding affinity of the ABD of plectin preceded by either exon 1a-, 1c-, or 1f-encoded sequences was found to be an order of magnitude higher than that of the ABD alone.[3] Thus, in addition to their proposed targeting function (17), some of plectin's first exon-encoded sequences might regulate the structural flexibility of the ABD of plectin, mediating conformational transitions required for its binding to various proteins, CaM included. In fact, ABDs of plectin modulated in that way may acquire specific binding properties that distinguish them from other isoforms. It remains to be shown in future experiments whether and how first exon-encoded sequences effect conformational changes of the ABD of plectin.

[3] J. Kostan, M. Gregor, G. Walko, and G. Wiche, unpublished data.

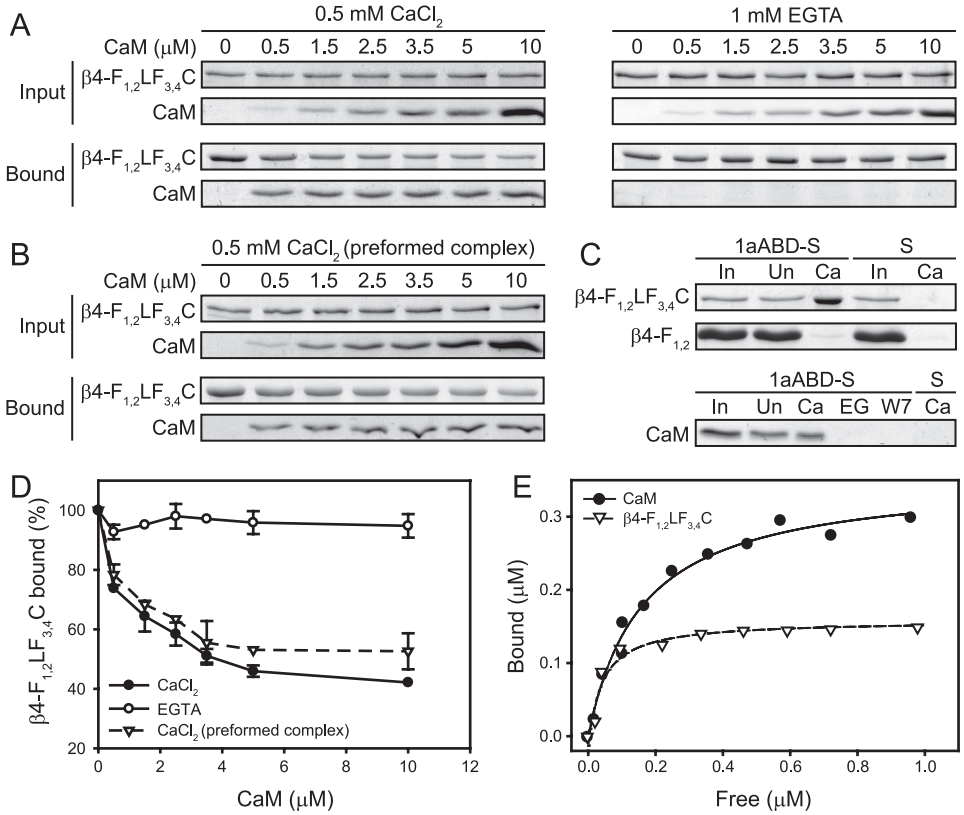

FIGURE 8. **CaM-dependent binding of integrin β4 to Sepharose bead-immobilized plectin fragment 1aABD.** *A*, mixtures of integrin β4 fragment β4-$F_{1,2}LF_{3,4}C$ (1.5 μM) and Sepharose bead-immobilized plectin 1aABD were incubated with increasing amounts of CaM (0–10 μM), in the presence (0.5 mM $CaCl_2$) or absence (1 mM EGTA) of Ca^{2+}. Proteins bound were analyzed by SDS-PAGE and visualized by CBB staining (*bound*). Aliquots of reaction mixtures taken prior to incubation were run as loading controls (*input*). *B*, as in *A*, except that intergrin/1aABD mixtures were incubated for 30 min prior to addition of CaM to preform a complex. *C*, integrin β4 fragments β4-$F_{1,2}LF_{3,4}C$ and β4-$F_{1,2}$ (*upper rows*), or CaM (*lower row*) were incubated with Sepharose bead-immobilized plectin 1aABD (*1aABD-S*) or empty beads (*S*) under the conditions indicated. *Ca*, 0.5 mM $CaCl_2$; *EG*, 1 mM EGTA; *W7*, 0.5 mM $CaCl_2$ and 80 μM W7. ~3% of reaction input (*In*) and of unbound protein (*Un*) were run as internal controls. Binding was analyzed as in *A*. *D*, 1aABD-bound β4-$F_{1,2}LF_{3,4}C$ fractions from *A* and *B* were determined by densitometric analysis of gels. Percent binding compared with that in the absence of CaM (100%) is shown. Data represent mean values (±S.E.) of three independent experiments. *E*, Sepharose bead-immobilized plectin 1aABD was incubated with increasing amounts of CaM, or β4-$F_{1,2}LF_{3,4}C$, in the presence of 0.5 mM $CaCl_2$. The amounts of free and bound proteins were determined by densitometric analysis of CBB-stained SDS-PAGE gels loaded with supernatant and pellet fractions similar to those shown in *C*. Data represent mean values of three independent experiments. Nonlinear regression analysis yielded average apparent K_d values of 0.16 and 0.05 μM, for CaM- and β4-$F_{1,2}LF_{3,4}C$-binding to 1aABD-Sepharose, respectively.

Implications of CaM Binding for Plectin-F-actin Interaction—Although CaM binding to the ABD of plectin 1a is likely to be of importance for the disassembly of HDs during keratinocyte differentiation (by preventing interaction with integrin β4), it remains to be seen whether CaM inhibition of actin binding has a biological function in this process as well. However, CaM-mediated regulation of this interaction may play a role in migration and terminal differentiation of keratinocytes. For instance, prevention of plectin-actin association by CaM could be a mechanism regulating actin reorganization and remodeling, which are required for the formation of cell protrusions during migration. Consistent with such notion, we have shown that plectin-deficient keratinocytes, lacking keratin-integrin α6β4 anchorage, have an elevated migration potential (27). PKC phosphorylation has been identified as another mechanism for the mobilization of integrin α6β4 from HDs and its association with F-actin in cellular protrusions of squamous carcinoma-derived A431 cells (39). Because we found CaM to associate with plectin 1a in the early stages of keratinocyte differentiation, prevention of plectin-actin interaction involving CaM might be important not only for actin remodeling, but also for modulating competitive actin-binding of plectin and integrin. In addition, in line with recent studies revealing a role of plectin as a scaffolding platform for proteins involved in signaling, the release of plectin from HDs and actin filaments mediated by PKC/CaM may be important for proper localization of signaling molecules involved in actin reorganization and remodeling during cell migration, particularly as plectin 1a was found to co-localize with CaM in cell protrusions after Ca^{2+} treatment of subconfluent keratinocytes culture. In confluent cultures, the release of plectin from HDs, along with inhibition of plectin-actin binding could possibly favor association of plectin with desmosomes, whose formation in keratinocytes is stimulated by Ca^{2+}. In fact, in confluent monolayers of differentiating keratinocytes our data showed redistribution of plectin 1a from HDs to the cell periphery in areas of cell-cell contacts. In line with this, plectin was found to be involved in the anchorage of IFs at desmosomes and the submembrane skeleton in polarized MDCK cells (42). More experiments will be necessary to fully explore this process.

Similar Fates of Plectin 1a and Integrin α6β4 during Keratinocyte Differentiation and Wound Healing—Our data showed that at late stages of Ca^{2+}-induced differentiation of keratinocytes there was a selective loss of plectin 1a, followed by down-regulation of its mRNA. A similar down-regulation has been reported for integrin α6β4, starting already at earlier stages of differentiation (25). In contrast, overexpression of both proteins has been observed, in processes involving transient changes in Ca^{2+} levels, like carcinoma invasion (43, 44) and wound healing (45). These findings suggest that Ca^{2+}-dependent regulation of hemidesmosomal protein levels is a general phenomenon.

Upon wounding a temporal increase in Ca^{2+} leads to the disassembly of HDs, a prerequisite for cell migration. However, during re-epithelization of the wound, the concentration of Ca^{2+} decreases and new cell-substrate contacts are formed, requiring the recirculation of plectin and integrin α6β4 and/or up-regulation of their expression. In line with this model, we found that the release of plectin 1a from HDs in

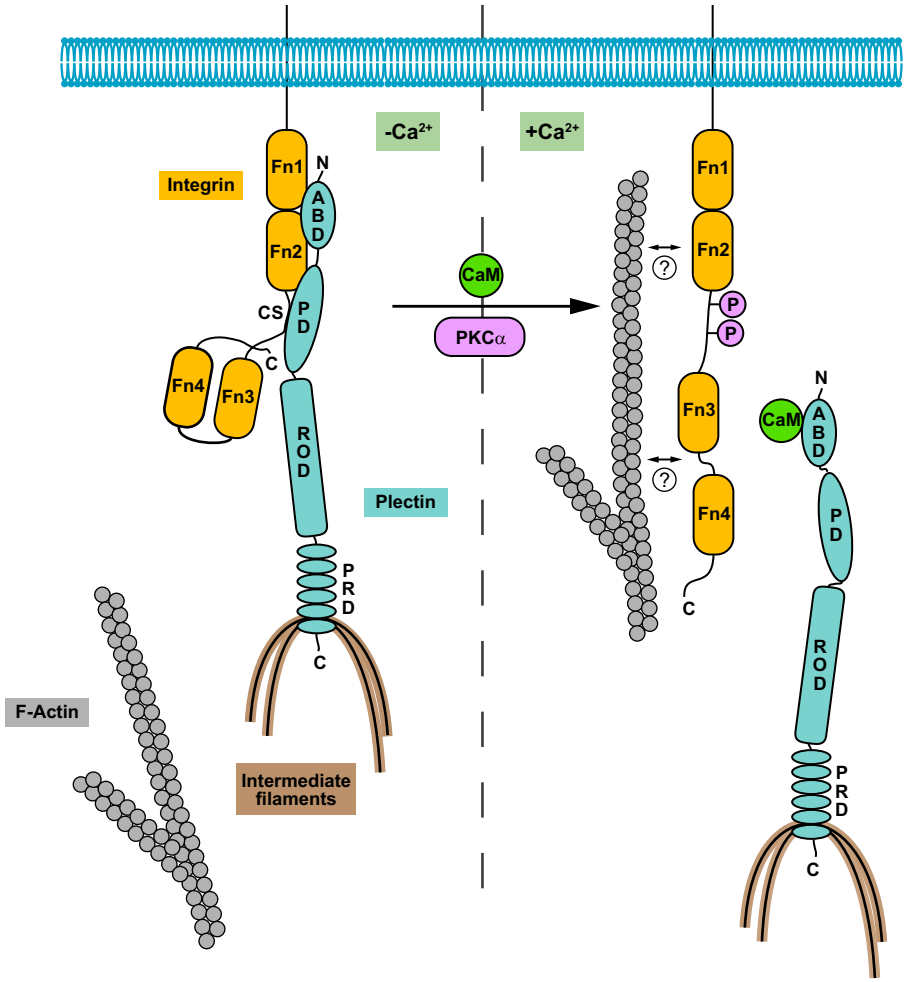

FIGURE 9. **Model of integrin-keratin linkage via plectin 1a in undifferentiated and Ca^{2+}-differentiated keratinocytes.** Under normal conditions ($-Ca^{2+}$), plectin 1a anchors IFs to HDs via association of its plakin domain (*PD*) with the connecting segment (*CS*) of integrin β4 and of its ABD with the first pair of the fibronectin type III (*Fn1* and *Fn2*) domains of integrin β4. When the concentration of Ca^{2+} in the cell increases ($+Ca^{2+}$), activation of PKCα leads to phosphorylation of serines within the CS domain of integrin, while CaM in its Ca^{2+}-bound form interacts with the ABD of plectin. Both events cause the dissociation of plectin from membrane-bound integrin and a redistribution of both proteins to actin-rich peripheral protrusions (and to perinuclear regions in the case of plectin). While integrin β4 might interact (directly or indirectly) with F-actin in such protrusions, as suggested by previous studies (39), the role of CaM remaining bound to the ABD of plectin could be to prevent it from interacting not only with integrin but also with F-actin, thereby disconnecting IFs from the membrane. Furthermore, with progressing differentiation, down-regulation of plectin 1a and integrin α6β4 expression occurs. Note that the previously reported interactions of plectin's C-terminal domain with the CS and tail domains of integrin β4 (for details see Ref. 9) are not shown (regulatory mechanisms involved in these interactions are unknown; however, CS phosphorylation might lead to destabilization of these interactions as well).

the early stages of keratinocyte differentiation, similar to the relocalization of plectin observed during wound healing (45), results in a redistribution of the protein within the cell, but not in its down-regulation. Furthermore, we observed that the bulk of the protein remained associated with the keratin filament network during this process, consistent with the role of plectin as a major organizing and stabilizing element of keratinocyte IF network cytoarchitecture (27). On the other hand, the long lasting exposure of cells to Ca^{2+}, mediated by physiological ion gradients within the epidermis (increasing from 0.5 mM in the basal layer to >1.4 mM in stratum granulosum) drives keratinocytes toward differentiation, terminated by programmed cell death. Because cell-matrix interactions are not required in the upper layers of the epidermis, down-regulation of hemidesmosomal components occurs, a process that at least in the case of plectin is likely to be mediated by caspases (46).

Recruitment of CaM Interferes with Plectin 1a-Integrin β4 Binding—It has been shown previously that EGF-triggered phosphorylation of integrin α6β4 by PKCα (23, 34) and/or Fyn (22) promotes the disassembly of HDs. Based on these observations, a mechanism of phosphorylation-induced HD disruption has been proposed (2). In our study an additional mechanism involved in this process has been uncovered, where Ca^{2+}-triggered binding of CaM to the ABD of plectin prevents its association with integrin β4. Taking both mechanisms into account, we propose a new model for the disassembly of the plectin-integrin α6β4 complex during keratinocyte differentiation (Fig. 9). In this model Ca^{2+}-trigged CaM binding to plectin and phosphorylation of integrin β4 by Ca^{2+}-activated PKCα play complementary roles. Thus, upon exposure of keratinocytes to Ca^{2+} during differentiation, both mechanisms are activated contributing to efficient disassembly of the plectin-integrin α6β4 complex and a redistribution of both subcomponents to actin-rich protrusions. There, the integrin may be associated with actin filaments (39), whereas plectin-actin interaction is prevented by CaM. Whether phosphorylation of integrin β4 precedes and/or is important for CaM binding to plectin, or whether additional regulatory factors are involved, remains to be shown. PKCα and CaM may act sequentially, or synergistically, one enhancing the effect of the other. Regulation could even be more complex, considering that phosphatidylinositol 4,5-bisphosphate, which was found to inhibit the interaction of the ABD of plectin with actin (47), binds to the CH2 domain of plectin, which in turn has been shown to be involved in plectin interaction with integrin β4 (2, 8). However, the role of phosphatidylinositol 4,5-bisphosphate in regulating plectin-integrin interaction has not been elucidated thus far.

In conclusion, we found CaM to participate in the regulation of HD disassembly by direct and Ca^{2+}-dependent binding to plectin 1a, thereby preventing plectin-integrin β4 association. CaM was found to regulate plectin-F-actin binding in a similar

manner. These mechanisms have important implications for keratinocyte differentiation, wound healing, and cell migration. Moreover, our study provided new insights into the molecular mechanism of how first exon-encoded sequences of plectin can modulate the functions of this unusually versatile cytolinker protein.

Acknowledgments—We thank Donald C. Chang (Hong Kong University, China), Maria Nemethova and Victor J. Small (both Institute of Molecular Biotechnology, Vienna), and Gerald Burgstaller (this laboratory) for the donation of plasmids.

REFERENCES

1. Jones, J. C., Hopkinson, S. B., and Goldfinger, L. E. (1998) *BioEssays* **20,** 488–494
2. Litjens, S. H., de Pereda, J. M., and Sonnenberg, A. (2006) *Trends Cell Biol.* **16,** 376–383
3. Wiche, G., Krepler, R., Artlieb, U., Pytela, R., and Aberer, W. (1984) *Exp. Cell Res.* **155,** 43–49
4. Wiche, G. (1998) *J. Cell Sci.* **111,** 2477–2486
5. Elliott, C. E., Becker, B., Oehler, S., Castañón, M. J., Hauptmann, R., and Wiche, G. (1997) *Genomics* **42,** 115–125
6. García-Alvarez, B., Bobkov, A., Sonnenberg, A., and de Pereda, J. M. (2003) *Structure* **11,** 615–625
7. Sevcík, J., Urbániková, L., Kost'an, J., Janda, L., and Wiche, G. (2004) *Eur. J. Biochem.* **271,** 1873–1884
8. Geerts, D., Fontao, L., Nievers, M. G., Schaapveld, R. Q., Purkis, P. E., Wheeler, G. N., Lane, E. B., Leigh, I. M., and Sonnenberg, A. (1999) *J. Cell Biol.* **147,** 417–434
9. Rezniczek, G. A., de Pereda, J. M., Reipert, S., and Wiche, G. (1998) *J. Cell Biol.* **141,** 209–225
10. Koster, J., van Wilpe, S., Kuikman, I., Litjens, S. H., and Sonnenberg, A. (2004) *Mol. Biol. Cell* **15,** 1211–1223
11. Pfendner, E., Rouan, F., and Uitto, J. (2005) *Exp. Dermatol.* **14,** 241–249
12. Koss-Harnes, D., Høyheim, B., Anton-Lamprecht, I., Gjesti, A., Jørgensen, R. S., Jahnsen, F. L., Olaisen, B., Wiche, G., and Gedde-Dahl, T., Jr. (2002) *J. Invest. Dermatol.* **118,** 87–93
13. Andrä, K., Lassmann, H., Bittner, R., Shorny, S., Fässler, R., Propst, F., and Wiche, G. (1997) *Genes Dev.* **11,** 3143–3156
14. Ackerl, R., Walko, G., Fuchs, P., Fischer, I., Schmuth, M., and Wiche, G. (2007) *J. Cell Sci.* **120,** 2435–2443
15. Fuchs, P., Zörer, M., Rezniczek, G. A., Spazierer, D., Oehler, S., Castañón, M. J., Hauptmann, R., and Wiche, G. (1999) *Hum. Mol. Genet.* **8,** 2461–2472
16. Andrä, K., Kornacker, I., Jörgl, A., Zörer, M., Spazierer, D., Fuchs, P., Fischer, I., and Wiche, G. (2003) *J. Invest. Dermatol.* **120,** 189–197
17. Rezniczek, G. A., Abrahamsberg, C., Fuchs, P., Spazierer, D., and Wiche, G. (2003) *Hum. Mol. Genet.* **12,** 3181–3194
18. Rezniczek, G. A., Konieczny, P., Nikolic, B., Reipert, S., Schneller, D., Abrahamsberg, C., Davies, K. E., Winder, S. J., and Wiche, G. (2007) *J. Cell Biol.* **176,** 965–977
19. Konieczny, P., Fuchs, P., Reipert, S., Kunz, W. S., Zeöld, A., Fischer, I., Paulin, D., Schröder, R., and Wiche, G. (2008) *J. Cell Biol.* **181,** 667–681
20. Winter, L., Abrahamsberg, C., and Wiche, G. (2008) *J. Cell Biol.* **181,** 903–911
21. Margadant, C., Frijns, E., Wilhelmsen, K., and Sonnenberg, A. (2008) *Curr. Opin. Cell Biol.* **20,** 589–596
22. Mariotti, A., Kedeshian, P. A., Dans, M., Curatola, A. M., Gagnoux-Palacios, L., and Giancotti, F. G. (2001) *J. Cell Biol.* **155,** 447–458
23. Wilhelmsen, K., Litjens, S. H., Kuikman, I., Margadant, C., van Rheenen, J., and Sonnenberg, A. (2007) *Mol. Biol. Cell* **18,** 3512–3522
24. Kitajima, Y., Owaribe, K., Nishizawa, Y., Jokura, Y., and Yaoita, H. (1992) *Exp. Cell Res.* **203,** 17–24
25. Tennenbaum, T., Li, L., Belanger, A. J., De Luca, L. M., and Yuspa, S. H. (1996) *Cell Growth Differ.* **7,** 615–628
26. Nikolic, B., Mac Nulty, E., Mir, B., and Wiche, G. (1996) *J. Cell Biol.* **134,** 1455–1467
27. Osmanagic-Myers, S., Gregor, M., Walko, G., Burgstaller, G., Reipert, S., and Wiche, G. (2006) *J. Cell Biol.* **174,** 557–568
28. Rezniczek, G. A., Janda, L., and Wiche, G. (2004) *Methods Cell Biol.* **78,** 721–755
29. Osmanagic-Myers, S., and Wiche, G. (2004) *J. Biol. Chem.* **279,** 18701–18710
30. Toivola, D. M., Zhou, Q., English, L. S., and Omary, M. B. (2002) *Mol. Biol. Cell* **13,** 1857–1870
31. Gopalakrishna, R., and Anderson, W. B. (1982) *Biochem. Biophys. Res. Commun.* **104,** 830–836
32. Spudich, J. A., and Watt, S. (1971) *J. Biol. Chem.* **246,** 4866–4871
33. Gipson, I. K., Spurr-Michaud, S., Tisdale, A., Elwell, J., and Stepp, M. A. (1993) *Exp. Cell Res.* **207,** 86–98
34. Rabinovitz, I., Tsomo, L., and Mercurio, A. M. (2004) *Mol. Cell. Biol.* **24,** 4351–4360
35. Bonet-Kerrache, A., Fabbrizio, E., and Mornet, D. (1994) *FEBS Lett.* **355,** 49–53
36. Winder, S. J., and Kendrick-Jones, J. (1995) *FEBS Lett.* **357,** 125–128
37. Nakamura, F., Hartwig, J. H., Stossel, T. P., and Szymanski, P. T. (2005) *J. Biol. Chem.* **280,** 32426–32433
38. Jarrett, H. W., and Foster, J. L. (1995) *J. Biol. Chem.* **270,** 5578–5586
39. Rabinovitz, I., Toker, A., and Mercurio, A. M. (1999) *J. Cell Biol.* **146,** 1147–1160
40. Santoro, M. M., Gaudino, G., and Marchisio, P. C. (2003) *Dev. Cell* **5,** 257–271
41. Litjens, S. H., Koster, J., Kuikman, I., van Wilpe, S., de Pereda, J. M., and Sonnenberg, A. (2003) *Mol. Biol. Cell* **14,** 4039–4050
42. Eger, A., Stockinger, A., Wiche, G., and Foisner, R. (1997) *J. Cell Sci.* **110,** 1307–1316
43. Lee, K. Y., Liu, Y. H., Ho, C. C., Pei, R. J., Yeh, K. T., Cheng, C. C., and Lai, Y. S. (2004) *J. Med.* **35,** 141–149
44. Janes, S. M., and Watt, F. M. (2006) *Nat. Rev. Cancer* **6,** 175–183
45. Stepp, M. A., Zhu, L., and Cranfill, R. (1996) *Invest. Ophthalmol. Vis. Sci.* **37,** 1593–1601
46. Stegh, A. H., Herrmann, H., Lampel, S., Weisenberger, D., Andrä, K., Seper, M., Wiche, G., Krammer, P. H., and Peter, M. E. (2000) *Mol. Cell. Biol.* **20,** 5665–5679
47. Andrä, K., Nikolic, B., Stöcher, M., Drenckhahn, D., and Wiche, G. (1998) *Genes Dev.* **12,** 3442–3451